

Equilibrium phases surrounding the α Zr solid solution in the Zr–Sn–O system

S. F. ARICÓ, L. M. GRIBAUDO, L. A. ROBERTI

Centro Atómico Constituyentes, Comisión Nacional de Energía Atómica, Avda. del Libertador 8250, Buenos Aires, 1429, República Argentina

Phases in equilibrium with the α Zr solid solution from 1014–1314 °C (1287–1587 K) in zirconium–tin–oxygen alloys were characterized and their compositions were determined. The experimental results provide information on the equilibria of the α Zr solid solution in order to propose tentative boundaries at isothermal sections of the phase diagram.

1. Introduction

Tin is the main element alloyed to zirconium in Zircaloy, a material very often used in nuclear reactors. This component widens, both in temperature and composition, the field of existence of the hcp solid solution α Zr at the expense of the bcc solid solution β Zr. Oxygen is also an α Zr-forming element and it is usually found in Zircaloy as an interstitial component at concentrations lower than 10000 at p.p.m. This consideration emphasizes the technological importance of the Zr–Sn–O system and the reasons for studying this subject in order to increase knowledge about the equilibria.

Data on the phase equilibria of the system Zr–Sn–O are very scarce; a summary of a review of the accessible literature is presented here, and available information about the metallic oxide sub-system zirconia–cassiterite (ZrO_2 – SnO_2) is also included.

The transformation temperatures $\alpha\text{Zr} \rightleftharpoons \beta\text{Zr}$ of several Zr–Sn alloys with low oxygen contents were presented by Arias and Roberti [1]. The results were obtained from resistivity measurements and they were corroborated by metallographic observations on specimens annealed for long times. Roberti [2] presented a tentative scheme for the phase boundaries between the α Zr, β Zr and Zr_4Sn phases at 970 and 1010 °C for oxygen plus nitrogen contents between 0 and 10000 at p.p.m.

Kwon and Corbett [3] reported the phases which are present in specimens treated at 1050 °C for 7 days in several Zr–Sn–O compositions obtained from arc-melted alloys made from zirconium, $\text{ZrO}_{0.1}$ and tin and sintered zirconium plus $\text{Zr}_5\text{Sn}_3\text{O}_x$ powders. The final bulk oxygen composition in the alloys ranged from 0.66–7.4 at % and the tin composition remained practically constant around 19.2 at % (18.5–19.9 at %).

Tsuji *et al.* [4] measured the heat capacity from 52–632 °C in two series of ternary Zr–Sn–O alloys containing 14.5 and 21.9 O at % and a tin composition between 0.0 and 5.5 at % Sn. While working experimentally on the metallic oxide sub-system,

Stöcker and Collongues [5] determined the maximum solubility of ZrO_2 in SnO_2 between 800 and 1300 °C to be 19 mol %, and the maximum solubility of SnO_2 in ZrO_2 at 800 °C to be 10 mol %. These authors found a metastable compound with orthorhombic structure at equimolecular amounts of the oxides. They obtained the metastable ZrSnO_4 as an amorphous precipitate, through coprecipitation by ammonia in boiling aqueous solutions. Collins and Ferguson [6] measured the lattice parameters of several solutions of SnO_2 in ZrO_2 on specimens as prepared by Stöcker and Collongues [5] and reported a maximum SnO_2 solubility in ZrO_2 of 14.7 mol %. Wilson and Glasser [7] found that the metastable phase ZrSnO_4 prepared at 1550 °C exsolves on prolonged annealing at 1500 °C to two distinct phases with average compositions of 10 and 82 mol % SnO_2 respectively.

The present paper reports the experimental determinations of the phases at equilibrium with the α Zr solid solution in the ternary Zr–Sn–O. These results, and those published by others, were used to outline the composition domain of this phase at temperatures between 1014 and 1314 °C.

Updated versions of the extreme binary phase diagrams used here are, for the O–Zr system, from Abriata *et al.* [8] and, for the Sn–Zr system, from Abriata *et al.* [9]. No phase diagram for the ZrO_2 – SnO_2 sub-system was found. Langeron [10], however, using some compiled information, proposed that this diagram should be analogous to the ZrO_2 – TiO_2 system.

2. Experimental procedure

2.1. Materials

The studied alloys were produced from the following materials: a zirconium-based alloy with 1.2 Sn at % (Fe < 650 at p.p.m., O < 7700 at p.p.m. and N < 350 at p.p.m.), pure tin with purity > 99.999%, and pure ZrO_2 with purity > 99%. These starting materials were labelled A1, A2 and A3, respectively.

2.2. Preparation

Specimens of about 12 g of different compositions were fabricated in a small arc-furnace with a tungsten electrode and a copper crucible in a highly pure argon atmosphere. To ensure homogeneity, the buttons were remelted at least four times. As the evaporation temperature of tin is 400 °C lower than the melting point of ZrO₂, two intermediate alloys were produced in order to avoid loss of tin during fabrication: Zr-0.7 Sn at %–40 O at % (A4), and Zr-17 Sn at % (A5), from A1, A2 and A3 alloys. The final compositions of the alloys are shown in Table I.

2.3. Heat treatments

Specimens wrapped in sheets of tantalum were placed under an argon atmosphere in quartz capsules which were previously carefully cleaned. All specimens were heat treated at 1014, 1304 and 1314 ± 2 °C for 813, 26 and 136 h, respectively. After these treatments, the samples were quenched in cold water.

2.4. Phase characterization

For the microscopic observations, both in optic (Reichert-MEV) and scanning electron equipment (Philips PSEM-500), the samples were polished and attacked with solution reagents in distilled water, 45% NO₃H plus 5% FH (for αZr and αZrO₂) and 20% NO₃H plus 20% FH (for Zr₅Sn₃).

The phases were identified by X-ray analysis (PW3710 based Philips) using monochromatic CuK_α radiation.

Composition analyses were made in the electron microprobe (Cameca SX50) at 20 keV accelerating voltage. The quantitative analyses were made after calibration with appropriate standards of zirconium (99.99% purity) and tin (99.999% purity) for the metals, and ZrO₂ (99% purity) for the oxygen. All elements (zirconium, tin and oxygen) were measured in each analysis.

3. Results

3.1. Metallographic analysis

Fig. 1 shows some representative micrographs of the structures of the alloys from the as-cast (Fig. 1a) to the heat-treated (Fig. 1b at 1014 °C and Fig. 1c at 1304 °C) conditions. The as-cast original structure of alloy M exhibits dendrites of the monoclinic αZrO₂,

TABLE I Compositions of the alloys

Specimen	Composition (at %)			Made from alloy
	Zr	Sn	O	
J	45.70	4.20	50.10	A3 + A5
K	68.10	11.90	20.00	A3 + A5
L	60.80	22.20	17.00	A2 + A3 + A5
M	55.90	6.90	37.20	A2 + A4
N	51.00	15.00	34.00	A2 + A4
O	48.80	18.70	32.50	A2 + A4

smooth Zr₅Sn₃ areas and small zones of hexagonal solid solution αZr(O, Sn). This structure evolved, after treatment, to a more definite and homogeneous one maintaining the same original solidified phases. The other alloys (J, K, L, N and O) present similar phases the only difference found being in the relative amounts.

3.2. X-ray spectroscopy

X-ray diffraction patterns showing the principal peaks of alloys M, N and O, heat treated at 1304 °C, are

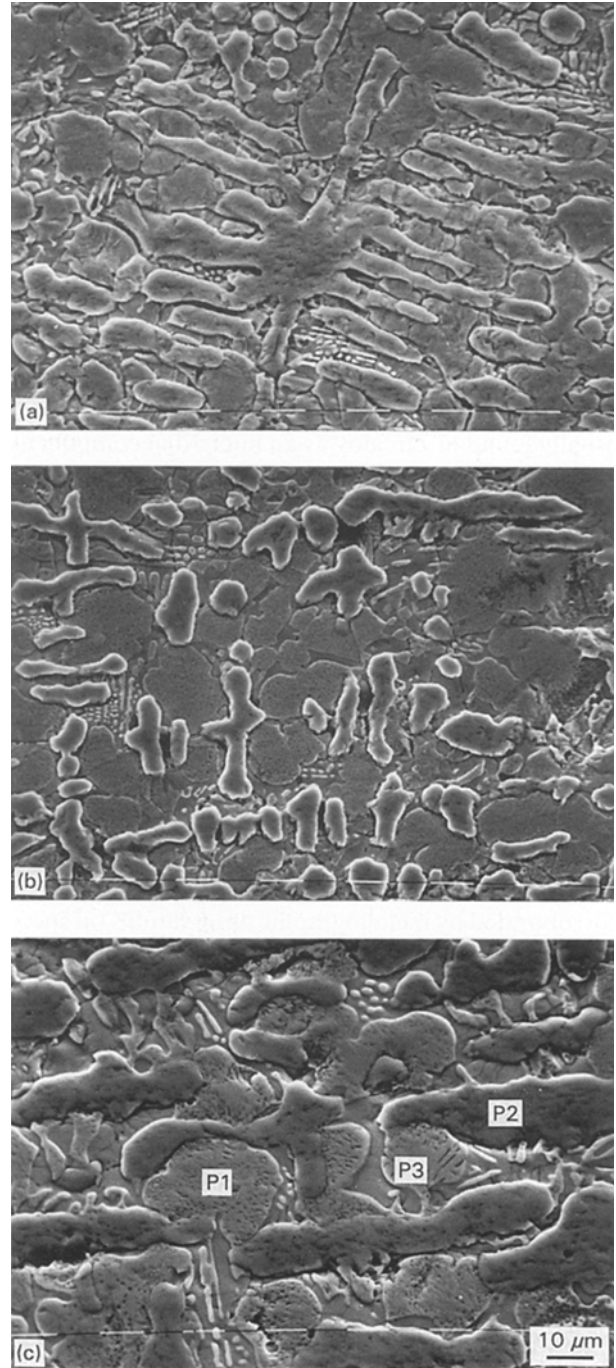


Figure 1 Electron micrographs of alloy M. (a) As-cast. Dendrites (αZrO₂), smooth areas (Zr₅Sn₃) and small zones of αZr(O, Sn). (b) Annealed (1014 °C for 813 h) and water quenched. (c) Annealed (1304 °C for 26 h) and water quenched. P1, evolved αZr(O, Sn); P2, globular αZrO₂; P3, Zr₅Sn₃.

presented in Fig. 2. All significant phases in a relatively important quantity were identified. From the patterns, and via careful identification of peaks and measurements, the parameters of the crystal structures were calculated for all alloys. Results are presented in Table II.

3.3. Phases in equilibrium

Table III summarizes the results of the identification of the phases by the three methods (metallographic,

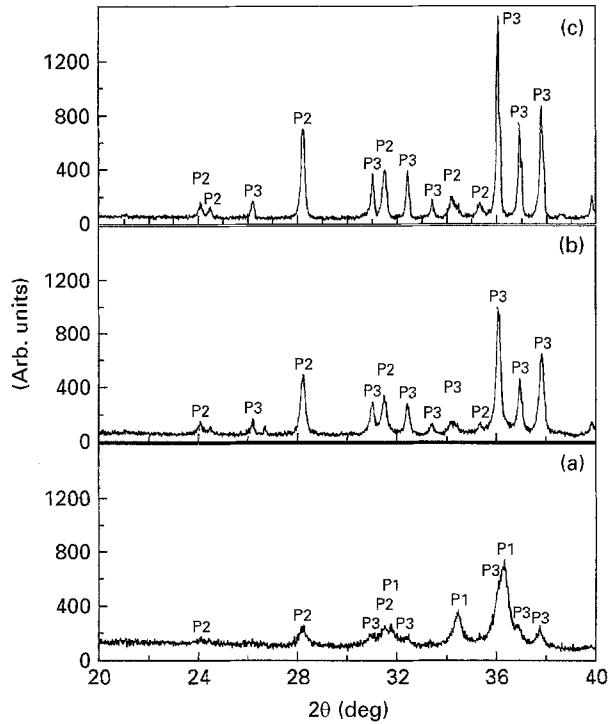


Figure 2 X-ray diffraction spectra for alloys (a) M and (b) N annealed at 1304°C and (c) O alloy annealed at 1314°C. P1, $\alpha\text{Zr}(\text{O}, \text{Sn})$; P2, αZrO_2 , P3, Zr_5Sn_3 .

TABLE II Lattice parameters

T (°C)	$\alpha\text{Zr}(\text{O}, \text{Sn})$			Zr_5Sn_3			From alloy
	a (nm)	c (nm)	c/a	a (nm)	c (nm)	c/a	
1014	0.3246	0.5201	1.602	0.8416	0.5788	0.688	J
	0.3242	0.5194	1.602	0.8420	0.5771	0.685	K
	0.3240	0.5195	1.604	0.8433	0.5767	0.684	L
1304	0.3244	0.5212	1.608	0.8408	0.5772	0.686	M
				0.8437	0.5770	0.684	N
1314				0.8418	0.5757	0.684	O

TABLE III Phases at equilibrium

Alloy	Heat treatment		
	1014°C, 813 h	1304°C, 26 h	1314°C, 136 h
J		$\alpha\text{Zr}(\text{O}, \text{Sn})-\alpha\text{ZrO}_2-\text{Zr}_5\text{Sn}_3$	
M			
K		$\text{Zr}_5\text{Sn}_3-\alpha\text{Zr}(\text{O}, \text{Sn})-\alpha\text{ZrO}_2$	
L			
N	$\text{Zr}_5\text{Sn}_3-\alpha\text{ZrO}_2-\alpha\text{Zr}(\text{O}, \text{Sn})$		$\text{Zr}_5\text{Sn}_3-\alpha\text{ZrO}_2-\alpha\text{Zr}(\text{O}, \text{Sn})$
O			$\text{Zr}_5\text{Sn}_3-\alpha\text{ZrO}_2$

quantitative electron-microprobe and X-ray diffraction). Taking into account the time-temperature conditions of the heat treatments, the microscopic observations and the partial results of the microprobe, it is considered that the phases are near the thermodynamic equilibrium. The arrangement in the table was made taking into account their relative quantities.

3.4. Phase composition

Results of the electron microprobe analysis are shown in Table IV. The estimated relative error of the measurements was less than 5%. The oxygen concentration was calculated from difference, but in each analysis the oxygen content was measured in a polished ZrO_2 button fabricated from pressed powers for an integrated reference and to ensure careful analysis of the phases which were in small amounts.

The oxygen content in the intermetallic Zr_5Sn_3 was zero. The metallic composition of this compound is constant for all alloys and very close to the stoichiometric amount (37.5 Sn at %).

ZrO_2 can dissolve a certain amount of SnO_2 but the measurements made in this work have shown that the quantities are lower than those published by Stöcker and Collongues [5].

4. Discussion

Results from the three methods of analysis applied (metallographic, quantitative electron-microprobe and X-ray diffraction) show that all the studied alloys submitted to isothermic heat treatments at 1014, 1304 and 1314°C, lay in a three-phase equilibrium domain between the solid solution $\alpha\text{Zr}(\text{O}, \text{Sn})$, the oxide αZrO_2 and the intermetallic Zr_5Sn_3 . The $\alpha\text{Zr}(\text{O}, \text{Sn})$ in the alloy labelled O treated at 1314°C was not discernible.

TABLE IV Compositions of phases at equilibrium

Alloy	Elements	Phases at equilibrium at each temperature					
		$\alpha\text{Zr(O,Sn)}$		Zr_5Sn_3		αZrO_2	
		1014 °C	1314 °C	1014 °C	1314 °C	1014 °C	1314 °C
J	Zr (at %)	68.6	70.2		62.9	33.45	
	Sn (at %)	2.0	1.3	■ ^a	37.1	0.05	F ^b
	O (at %)	29.4	28.5		0	66.5	
K	Zr (at %)	66.4	66.3	62.0	62.3		
	Sn (at %)	3.4	2.1	38.0	37.7	F ^b	F ^b
	O (at %)	30.1	31.7	0	0		
L	Zr (at %)		67.6	62.6	62.8		33.65
	Sn (at %)	■ ^a	1.6	37.4	37.2	F ^b	0.05
	O (at %)		30.8	0	0		66.3
M	Zr (at %)	67.8	68.2	62.8			35.45
	Sn (at %)	2.2	1.4	37.2	■ ^a	F ^b	0.05
	O (at %)	30.0	30.4	0			64.5
N	Zr (at %)		58.1		63.2		
	Sn (at %)	■ ^a	2.1	■ ^a	36.8	F ^b	F ^b
	O (at %)		39.8		0		
O	Zr (at %)	62.0		61.0	62.7	30.95	31.95
	Sn (at %)	3.5	—	39.0	37.2	0.05	0.05
	O (at %)	34.6		0	0	69.0	68.0

■^a, identified not measured.
F^b, identified from fluorescence.

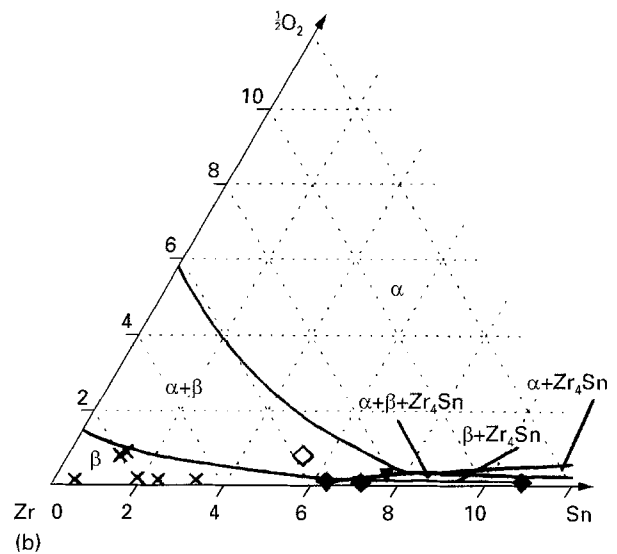
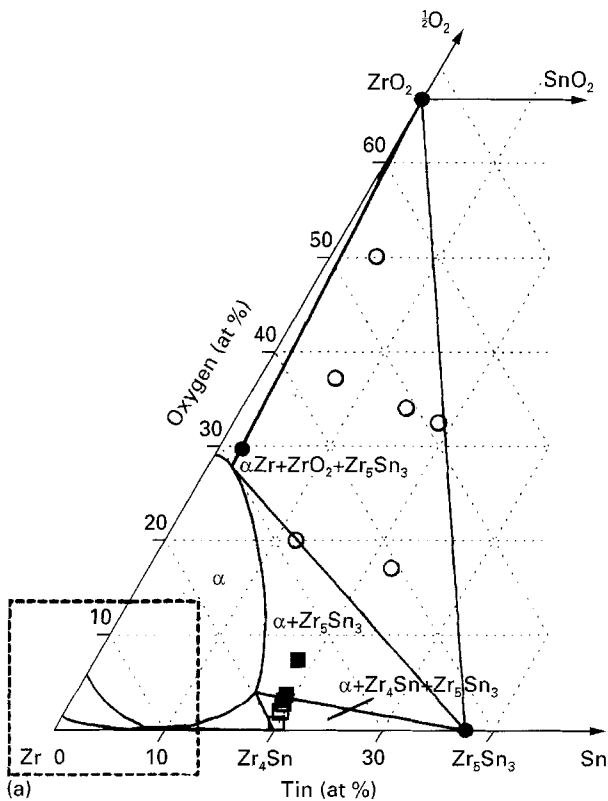


Figure 3 Equilibria surrounding the $\alpha\text{Zr(O,Sn)}$ phase at 1014 °C. (a) Proposed boundaries. (b) Enlarged view. (■) $\alpha\text{Zr} + \text{Zr}_5\text{Sn}_3$ [3]; (□) $\alpha\text{Zr} + \text{Zr}_4\text{Sn} + \text{Zr}_5\text{Sn}_3$ [3], (×) β [2], (◆) $\alpha\text{Zr} + \beta\text{Zr}$ [2], (◇) $\beta\text{Zr} + \text{Zr}_4\text{Sn}$ [2], (▼) $\alpha\text{Zr} + \beta\text{Zr} + \text{Zr}_4\text{Sn}$ [2], (○) $\alpha\text{Zr} + \text{Zr}_5\text{Sn}_3 + \text{ZrO}_2$ (present work). (—) Tentative boundaries, (●) averaged composition from microprobe analysis of αZr , αZrO_2 and Zr_5Sn_3 .

Fig. 3a shows the isothermal section at 1014 °C of the zirconium-rich zone of the Zr–Sn–O system. The initial composition of the alloys produced in this work, the compositions of the three phases obtained after treatment and considered at equilibrium, and the tentative boundaries proposed in this work, are marked in Fig. 3. Fig. 3b shows an enlarged zone for a better visualization of equilibria among the phases $\alpha\text{Zr(O,Sn)}$, $\beta\text{Zr(O,Sn)}$ and Zr_4Sn near the zirconium

corner. The experimental results of Roberti [2] at 1010 °C and those of Kwon and Corbett [3] at 1050 °C are also included in the figures.

The point 68.2 Zr at %–2.1 Sn at %–29.7 O at % was chosen to represent the $\alpha\text{Zr(O,Sn)}$ phase at equilibrium. This value is the average of the composition analysis of the phase in the J and M alloys, where the volume of the $\alpha\text{Zr(O,Sn)}$ was sufficiently large to ensure reliable measurements in the microprobe.

The point 62.1 Zr at %–37.9 Sn at %–0.0 O at % represents the intermetallic Zr_5Sn_3 in equilibrium at 1014 °C. This value is an average of the measurements on alloys K, L, M and O.

The point representing the αZrO_2 at equilibrium, 32.15 Zr at %–67.75 O at %–0.05 Sn at %, was taken from the average of the measurements in J and O alloys.

The solubility of SnO_2 in αZrO_2 when the phases $\alpha Zr(O, Sn)$, αZrO_2 and Zr_5Sn_3 are in equilibrium at 1014 °C is about 0.15 mol % (0.05 Sn at %). This value is low if compared to 3.3 mol % (1 Sn at %), which was obtained after interpolating in temperature the published data from Stöcker and Collongues [5] for 800 °C.

The lattice parameters in the hexagonal αZr are modified when tin and oxygen are added. Tin decreases a [11] and oxygen enlarges both a and c [12]. The results of this work, which show a certain constancy and independence of the composition in the $\alpha Zr(O, Sn)$ phase, agree with this opposed tendency.

The lattice parameters of the intermetallic Zr_5Sn_3 with Mn_5Si_3 -type structure, measured in several specimens of quenched alloys from 1014 and 1304 °C where the volume of the phase was different, are in a total agreement with the published values of Kwon and Corbett [13] obtained from sintered alloys at 1000 °C, those of Gran and Andersson [14] over alloys arc-melted and annealed at 900 °C, and those mentioned by Roberti [2] for the binary Zr–Sn alloys. The (Ti_5Ga_4 -type) Zr_5Sn_4 phase was never found in these ternary alloys, nor in the measurements of the composition analysis, nor the X-ray diffraction patterns, as reported by Kwon and Corbett [13].

Owing to the fact that the measured compositions of the $\alpha Zr(O, Sn)$, Zr_5Sn_3 and αZrO_2 phases in equilibrium at 1314 °C are very similar to those at 1014 °C the univariant three-phase triangle would not be modified and the general feature of this zone of the isothermal section diagram would be analogous.

5. Conclusions

1. The intermetallic compound Zr_5Sn_3 does not accept oxygen when it is in an equilibrium state in the Zr–Sn–O system.

2. The solubility of SnO_2 in ZrO_2 is low (about 0.15 mol %) when it exists in equilibrium with the $\alpha Zr(O, Sn)$ phase and the intermetallic Zr_5Sn_3 between 1014 and 1314 °C.

3. A three-phase equilibrium domain at 1014 °C was found, the related phases and their compositions being:

$\alpha Zr(O, Sn)$: 68.2 Zr at %–2.1 Sn at %–29.7 O at %, Zr_5Sn_3 : 62.1 Zr at %–37.9 Sn at %–0.0 O at %, and αZrO_2 : 32.15 Zr at %–0.05 Sn at %–67.75 O at %.

The equilibrium compositions of these three phases are practically the same at 1314 °C:

$\alpha Zr(O, Sn)$: 69.7 Zr at %–1.3 Sn at %–29 O at %, Zr_5Sn_3 : 62.8 Zr at %–37.2 Sn at %–0.0 O at %, and αZrO_2 : 33.65 Zr at %–0.05 Sn at %–66.3 O at %.

4. The results of this work were used in order to present a proposal of the tentative boundaries surrounding the αZr on the isothermal section diagram at 1014 °C.

5. The general feature of this zone of the diagram at 1314 °C would be similar to the 1014 °C section.

Acknowledgements

The present work was partially supported by the Consejo Nacional de Investigaciones Científicas y Técnicas (Argentina) under grant PIA-0015/92.

References

1. D. ARIAS and L. ROBERTI, *J. Nucl. Mater.* **118** (1983) 143.
2. L. ROBERTI, Doctoral Thesis, Universidad Nacional de Buenos Aires (1992) p. 89.
3. Y.-U. KWON and J. CORBETT, *Chem. Mater.* **4** (1992) 187.
4. T. TSUJI, M. AMAYA and K. NAITO, *J. Nucl. Mater.* **201** (1993) 126.
5. J. STÖCKER and R. COLLONGUES, *Compt. Rend.* **244** (1957) 83.
6. J. COLLINS and I. FERGUSON, *J. Chem. Soc. (A)* (1968) 4.
7. G. WILSON and F. GLASSER, *Trans. Br. Ceram. Soc.* **88** (1989) 69.
8. J. ABRIATA, J. GARCÉS and R. VERSACI, *Bull. Alloy Phase Diag.* **7** (1986) 116.
9. J. ABRIATA, J. BOLCICH and D. ARIAS, *ibid.* **4** (1983) 147.
10. J.-P. LANGERON, "Oxides de Zirconium" in "Nouveau Traité de Chimie Minérale", P. Pascal (ed), Vol. IX (Masson, Paris, 1963) p. 485.
11. J. BETTERTON Jr and D. EASTON, *J. Metals* **13** (1961) 86.
12. B. O. LICHTER, *Trans. Metall. Soc. AIME* **218** (1960) 1015.
13. Y.-U. KWON and J. D. CORBETT, *Chem. Mater.* **2** (1990) 27.
14. G. GRAN and S. ANDERSSON, *Acta Chem. Scand.* **14** (1960) 956.

Received 31 October 1995
and accepted 24 April 1996